DESIGN AND EXPERIMENTAL STUDY OF THE SUPPLY SYSTEM FOR GRASS SEED PELLETIZATION COATING MACHINE
/
草种丸粒化包衣机供给装置设计与研究

Liying CHEN[1], Zhanfeng HOU[*1,2,3], Haiyang LIU[1], Bingyan LI[1], Liyang BAO[1], Zhimin WANG[1]
[1] Inner Mongolia Agricultural University, College of Mechanical and Electrical Engineering, Inner Mongolia, China
[2] Inner Mongolia Engineering Research Center of Intelligent Equipment for the Entire Process of Forage and Feed Production, Hohhot, 010018, China
[3] Inner Mongolia Engineering Research Center for Intelligent Facilities in Prataculture and Livestock Breeding, Hohhot 010018, China
Tel: +86-0471-4309215; E-mail: njau-hzf@163.com
Corresponding author: Zhanfeng HOU
DOI: https://doi.org/10.35633/inmateh-75-96

***Keywords:** Pelletization Coating, Small-sized Forage Grass Seeds, Electronic Control System, Microcontroller Unit, Bidirectional Thyristor Circuit, Precision Dosage Control.*

ABSTRACT
To address the challenges of low automation, insufficient precision in seed-powder-liquid ratio control, and suboptimal coating quality in current domestic small-sized forage grass seed pelletization coating equipment, this study designed and developed a fully automated pelletization coating system. The system employs a Microcontroller Unit as the core controller, integrates an ATFC101 serial touchscreen for human-machine interaction, and combines programming and electronic control technologies to achieve precise regulation of material and liquid supply, enabling fully automated and quantized coating operations. The hardware of the feeding system adopts a bidirectional thyristor circuit, while the software implements a hierarchical switching control strategy to ensure high precision and stable material delivery. Experimental trials using Caragana seeds and pelletization powder demonstrated that the integrated electro-control system achieved full automation, with seed dispensing deviation controlled within 1.2 g and powder deviation within 0.32 g, significantly improving dosing accuracy. This research provides critical theoretical and technical insights for optimizing automated pelletization coating equipment for small-sized forage grass seeds.

摘要
针对当前国内小粒牧草种子丸化包衣设备存在的自动化程度低、种粉液比例控制精度不足及包衣质量欠佳等问题，本研究设计并开发了一种小粒牧草种子全自动丸化包衣设备，系统以单片机为核心控制器，采用ATFC101 串口屏作为人机交互界面，结合编程与电控技术，实现了供料与供液量的精确调控，进而达成全自动精量化包衣操作。供料系统硬件部分采用双向晶闸管电路，软件采用分层切换控制策略，确保了供料的高精度与稳定性。以柠条种子及丸粒化粉料为试验对象，研究结果表明，该电控系统与丸化包衣设备的集成实现了全自动操作，其中落种偏差控制在1.2g 以内，落粉偏差控制在0.32g 以内，显著提升了精确落料性能。本研究为小粒牧草种子全自动丸化包衣设备的设计与优化提供了重要的理论依据与技术参考。

INTRODUCTION
Seed pelletization coating technology is a processing method that uniformly encapsulates seeds with powdered agents, liquid binders, and other nutritional or protective materials to form small, spherical pellets with consistent size and shape. This technology not only significantly improves seed precision in mechanical precision seeding but also enhances seed resilience against biotic and abiotic stresses (*Jarrar et al., 2023; Paravar et al., 2023; Yi, 2020*). This technique has been widely applied in grassland ecological restoration projects to rehabilitate degraded and desertified grasslands through aerial seeding. By increasing seed size and mass, pelletization effectively mitigates the impact of wind speed and direction on seed dispersal, improves landing stability, and ensures better soil surface embedding, thereby substantially enhancing aerial seeding quality (*Pedrini et al., 2023; Zheng et al., 2024*). These benefits are particularly pronounced for small-sized forage grass seeds, which exhibit markedly improved germination rates and ecological adaptability post-treatment (*Javed et al., 2022*).

Pelletization coating technology originated internationally in the 1940s. Over nearly 80 years of advancement, equipment development has evolved from rudimentary mechanical operations to intelligent and precision-driven modern systems. For instance, Denmark's HEID Corporation produces the CC-type rotary seed coater, which utilizes automated control systems to precisely coordinate the metering of materials and coating agents, effectively minimizing human error and enhancing coating uniformity and pelletization quality. Canada's Ohara Technologies developed the HVCC3015 continuous coater, featuring a zone-controlled, multi-angle spray nozzle design that optimizes spray angles and chemical dosage, significantly reducing coating dead zones and improving uniformity, efficiency, and final product quality. With dynamic metering and modular design, Niklas Germany has developed W.N.14 continuous coating machine, which realizes precise proportioning and automated operation through metering roller linkage and PLC control to enhance coating uniformity, reduce pharmaceutical waste and improve production efficiency (*Ma et al., 2023*). In contrast, domestic research on pelletization in China began relatively late, transitioning from manual operations in the 1990s to fully automated systems. Chinese scholars have designed and tested pelletizers for diverse seed types while continuously optimizing their electro-control systems. Examples include the 5BY-5.0V Seed Coater by Jiuquan Okay Seed Co., which ensures precise chemical-to-seed ratios and thorough mixing. *Yang et al. (2014)* developed an intelligent control system to enhance coating quality and synchronize seed-chemical delivery. *Sang et al. (2015)* integrated advanced detection and control systems into the BY-150 coater, significantly improving dosing accuracy for both seeds and liquid agents. The 5BYR-100 Seed Coater, designed by the Guangdong Provincial Agricultural Machinery Research Institute, was optimized for batch coating of vegetable seeds. Despite these advancements, existing equipment predominantly targets vegetable and crop seeds, with limited options for small-sized forage grass seeds, and automation levels remain suboptimal. While researchers have improved pelletization quality through mechanical refinements, critical factors such as seed-powder-liquid ratios - key determinants of coating efficacy - are often inadequately addressed in current studies.

To address the aforementioned challenges, this study designed a fully automated pelletization coating system for small-sized forage grass seeds, achieving precise control over seed, powder, and liquid supply, alongside fully automated coating operations. Centered around a microcontroller unit and integrated with a closed-loop control strategy, the system enables intelligent regulation and stable operation throughout the entire process. This innovation aims to enhance the quality and efficiency of seed pelletization coating, providing robust technical support for forage cultivation and ecological restoration projects.

MATERIALS AND METHODS

Overall Structure and Operational Principle

System Architecture

The grass seed pelletization coating equipment consists of a powder feeding device, seed feeding device, liquid feeding device, pelletization coating device, and control system. Its structure is shown in Fig.1.

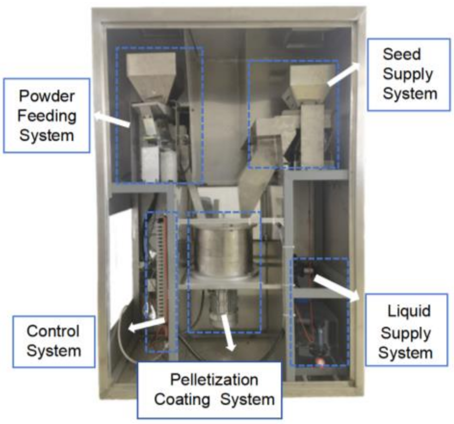

Fig. 1 – Schematic diagram of the overall system structure

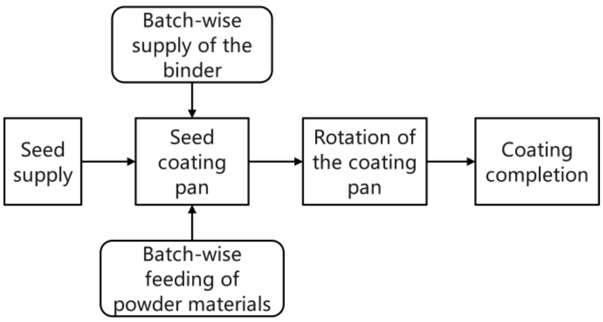

Fig. 2 – Flow chart of the pelletization process

The operational workflow of the pelletization coating equipment is as follows: First, the seed feeding device delivers seeds into the pelletization coating drum. After initiating drum rotation, the seeds are evenly distributed within the drum.

The liquid supply system then activates, injecting the coating solution into the drum. The drum continues rotating in an idle state to ensure thorough wetting of the seed surfaces. Subsequently, the powder feeding device supplies powdered material into the drum, followed by another idling phase to achieve uniform powder coating. Throughout the process, the liquid coating agent is supplied in quantitatively controlled batches, with powder dosing always synchronized after the liquid application. The batch-wise liquid and powder supply sequence is illustrated in Figure 2, operating in a cyclic "liquid supply-idling-powder supply-idling" mode until the preset pelletization criteria are met (*Pasha et al., 2017)*. Finally, the drum idles for an extended period to enhance the compressive strength and surface smoothness of the coated pellets, completing one full coating cycle.

Control Workflow Overview

Based on the operational workflow of the pelletization coating equipment, the overall control flowchart of the system was designed, as illustrated in Figure 3. After system startup, initialization is completed first. Subsequently, operational parameters are configured via the touchscreen, and the equipment is activated. The system initiates seed feeding and enters an idle operation state once the seed quantity reaches the preset value. After the idle operation time meets the set duration, the liquid supply process is triggered. When the liquid supply volume reaches the single-cycle target, the system halts the liquid supply and re-enters idle operation. Following this, the powder supply process is activated, succeeded by another idle phase. The system operates cyclically in the “liquid supply-idle operation-powder supply-idle operation” sequence until the predetermined number of cycles is achieved, after which it transitions to the pelletization phase. During pelletization, the system runs for the set duration, concluding the process. The equipment then stops, marking the completion of a full coating cycle.

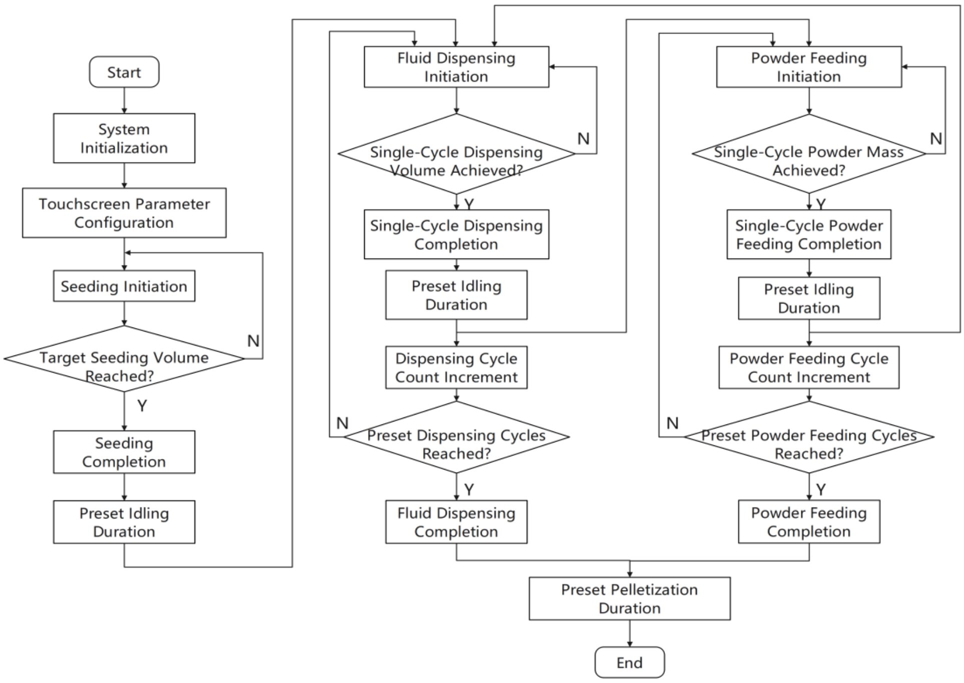

Fig. 3 – Control system flow diagram

Design of the Seed Supply Device

Structure and Working Process

A seed metering device was ultimately designed by integrating a load cell, servo motor, and weighing hopper into the electromagnetic vibratory feeder. The structure of the feeder, as shown in Figure 4, comprises a material trough, leaf springs, an electromagnetic vibratory exciter, a base frame, and vibration isolation springs *(Afzal et al., 2020)*. The electromagnetic exciter consists of critical components such as an electromagnet (coil with iron core) and an armature. In the alternating current (AC)-driven electromagnetic vibratory feeder, the operational principle relies on the coupling of electromagnetic forces and mechanical vibrations. When AC flows through the electromagnet coil, an alternating magnetic field is generated, producing periodic electromagnetic forces. During the positive half-cycle of the AC, current energizes the coil, creating an electromagnetic force that attracts the armature to the iron core. This action drives the trough backward while deforming the leaf springs to store elastic potential energy. During the negative half-cycle, the current direction reverses, weakening or eliminating the electromagnetic attraction.

The leaf springs then release stored energy, propelling the armature and iron core in the opposite direction, thereby moving the trough forward. With a standard AC frequency of 50 Hz, the feeder completes 50 reciprocating vibrations per second, equivalent to 3,000 cycles per minute (*Mucchi et al., 2013)*. This process converts electrical energy into mechanical energy through electromagnetic forces, enabling periodic vibrations of the trough to achieve material conveyance.

The feeding capacity of an electromagnetic vibratory feeder is influenced by multiple critical factors, including the mechanical index, trough inclination angle, and material properties (particle size, density, and moisture content). Among these, the mechanical index (*K*), defined as the ratio of the trough's maximum acceleration to gravitational acceleration, serves as a core parameter that directly governs material conveying speed and uniformity (*Despotović et al., 2017; Chandravanshi et al., 2017)*.

$$K = 4\pi^2 f^2 a / g \tag{1}$$

In the formula: f - vibration frequency, [Hz];

a - amplitude, [m];

g - gravitational acceleration, [m/s²].

In this study, the vibration frequency was set to 3,000 cycles per minute (50 Hz). By adjusting the vibration amplitude (*a*), the feeding capacity was optimized to accommodate the conveying requirements of diverse materials, thereby improving operational efficiency and precision. Building on this foundation, the electromagnetic vibratory feeder was enhanced and an intelligent seed feeding device was designed. This device enables two operational modes-high-speed and low-speed-by modulating the exciter’s amplitude: high-speed mode prioritizes feeding rate for rapid material delivery, while low-speed mode minimizes feeding error to ensure precise quantitative dosing.

During system operation, the seed supply system drives the trough vibration via the electromagnetic vibratory exciter in high-speed mode, conveying seeds to the weighing hopper. The Microcontroller Unit monitors the real-time seed weight in the hopper through feedback from the load cell. When the feeding rate reaches the switching point (expressed as a percentage of the total seed quantity), the Microcontroller Unit switches the exciter to low-speed mode to enhance dosing precision *(Zhang et al., 2021; Campos et al., 2012)*. Upon achieving the preset seed quantity, the Microcontroller Unit halts the exciter's vibration and controls the servo motor to rotate at a specified angle, thereby opening the discharge gate to deposit the quantified seeds into the pelletization coating drum. The process flowchart is illustrated in Figure 5.

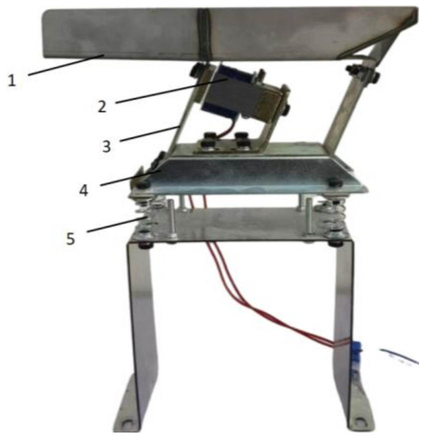

Fig. 4 – Structural diagram of the electromagnetic vibration feeder

1. material trough; 2. electromagnetic vibratory exciter; 3. leaf spring; 4. base frame; 5. vibration isolation spring

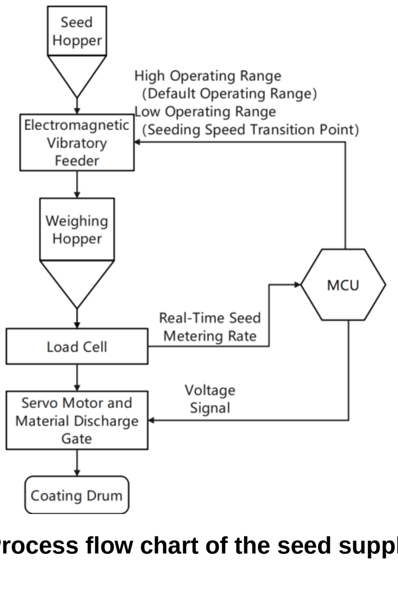

Fig. 5 – Process flow chart of the seed supply system

Hardware Design

The hardware components of the seed-feeding device primarily consist of a load cell, electromagnetic vibrator, and servo motor. To ensure precise seed delivery, the system employs a high-precision parallel cantilever load cell with a 0-2 kg range and 0.02 g accuracy. This load cell features a composite error of <0.02% F.S., an operational temperature range of -20 to +75°C, sensitivity of 1±0.03 mV/V, a power supply voltage of 5-12 V, and an overload capacity of 150% F.S., offering high accuracy, user-friendly operation, and strong anti-interference capability. Since the load cell's output signal is weak and susceptible to interference, the system incorporates an HX711 module to amplify and convert the analog signals.

This module integrates a high-precision 24-bit A/D converter with a 2.6-5.5 V operating voltage range, delivering low-noise, high-resolution performance for stable digital output, making it ideal for high-accuracy weighing applications.

The amplitude regulation of the electromagnetic vibrator is achieved through a TRIAC-based voltage control circuit (shown in Figure 6). This circuit connects the mains power to the signal input terminal, with the output terminal linked to the electromagnetic vibrator. The circuit configuration includes: Q1 as the bidirectional thyristor (TRIAC), D1 as the bidirectional trigger diode (DIAC), *RX*/R2/C2 forming the phase-shift network, and C1/R1 composing the snubber circuit to suppress voltage transients during switching operations and protect circuit components. By adjusting the resistance value (*RX*) in the phase-shift network, the circuit controls the charging time of capacitor C2 until it reaches the DIAC's trigger voltage (32 V), thereby modulating the TRIAC's conduction phase angle. This directly varies the output RMS voltage, enabling the electromagnetic vibrator to operate at two distinct speed settings (high/low) for seed feeding applications.

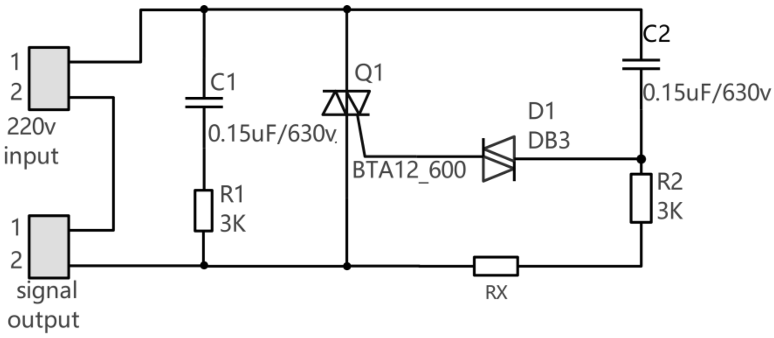

Fig. 6 –TRIAC voltage regulating circuit

The system employs a metal-gear micro servo with a 0.4413 N·m torque and a 180° controllable rotation range, featuring a no-load speed of 0.14s/60° at a 6V operating voltage. This servo provides precise angular positioning while maintaining excellent wear resistance and operational stability, ensuring consistent performance during prolonged high-frequency operation for rapid and accurate gate control in the feeding process. The servo is controlled through PWM signals with pulse widths ranging from 500 μs to 2500 μs (0.5-2.5 ms), where smaller pulse widths correspond to smaller rotation angles and larger pulses produce proportionally greater angles. This enables smooth 0-180° rotation for fine-tuned gate positioning, meeting the precise angular control requirements of the feeding system.

Design of the Powder Feeding Device

Although the material hoppers and specifications of the weighing system (hopper dimensions and weighing hopper capacity) differ between the powder feeding device and the seed feeding device, their mechanical structures, operational workflows, and hardware designs remain highly consistent. The process flowchart of the powder feeding system is illustrated in Figure 7.

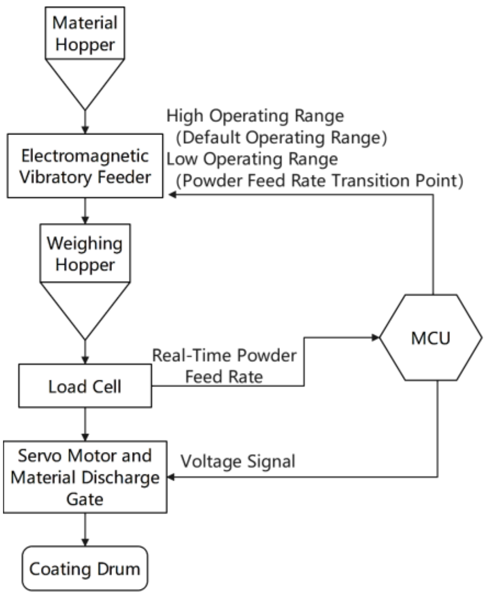

Fig. 7 – Process flow chart of the powder supply system

Design of the Liquid Delivery Device
Structure and Working Process

The liquid feeding system comprises a medicinal solution tank, a liquid supply pump, a flow meter, and an electromagnetic valve. The flow meter monitors the liquid flow rate in real-time and transmits the data to the Microcontroller Unit, enabling precise measurement and control of the liquid supply volume. The operational workflow is as follows: the liquid supply pump delivers the medicinal solution through a pipeline to the pellet coating pot, while the flow sensor continuously collects flow rate data and sends it back to the Microcontroller Unit. When the detected value reaches the preset threshold, the Microcontroller Unit immediately triggers a shutdown command to the electromagnetic valve, terminating the current liquid supply cycle. The process flow diagram of the liquid feeding system is illustrated in Figure 8.

Hardware Design

The hardware components of the liquid feeding system primarily consist of a liquid supply pump, flow meter, and solenoid valve. To ensure accurate flow measurement, the system employs a Digmesa flow meter with a measurement range of 0.05-0.82 L/min and an accuracy of ±0.5% F.S. This flow meter has a total error of less than 0.5% F.S., an operating temperature range of -10 to +60°C, output signals of 4-20mA or pulse, a power supply voltage of 12-24V DC, and an overload capacity of 120% F.S. With advantages such as high measurement accuracy, fast response speed, and strong resistance to medium contamination, it is particularly suitable for fluid control applications requiring low flow rates and high precision.

In the liquid feeding system, a normally closed DC 12V solenoid valve is installed at the outlet of the liquid supply pump to prevent backflow. Coupled with its dedicated driver circuit (shown in Figure 9), this solenoid valve allows for real-time, precise control of liquid flow. The driver circuit utilizes a high-response configuration consisting of a transistor-relay combination for accurate flow regulation. The control mechanism operates via the Microcontroller Unit's I/O port, which is connected to the solenoid valve driver circuit. When the I/O port outputs a high-level signal, the transistor enters saturation, energizing the relay to open the solenoid valve and initiate liquid flow. Conversely, a low-level signal from the I/O port drives the transistor into cutoff, de-energizing the relay to close the solenoid valve and stop the liquid flow. This switching mechanism provides reliable on/off control, with response times under 15ms, as confirmed through experimental testing.

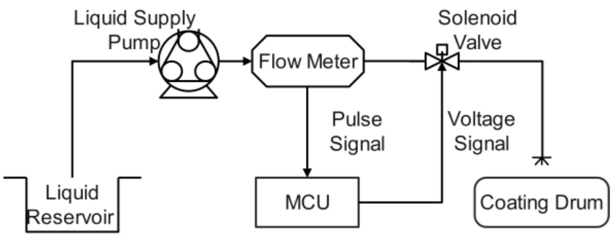

Fig. 8 – Process flow chart of the liquid supply system

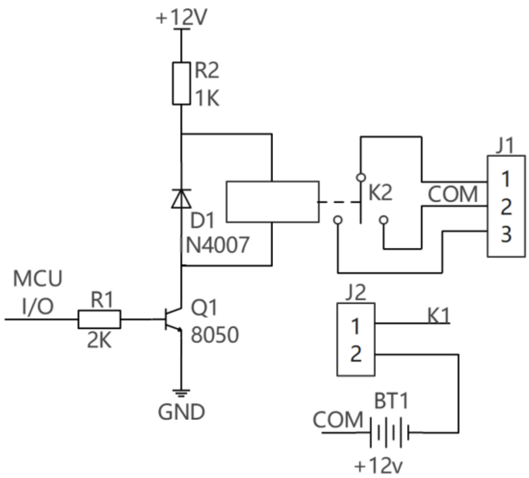

Fig. 9 – Driving circuit of the solenoid valve

Overall Control System Design

The small grass seed pelleting and coating equipment consists of a feeding device and a pelleting-coating unit. The pelleting-coating unit includes a speed sensor, frequency converter, AC motor, and coating drum. Based on closed-loop control principles, this study designed both the feeding device and pelleting-coating unit, with the closed-loop control system structure shown in Figure 10 (*Upasan et al., 2013; Gai et al., 2013)*. In this system, sensors continuously collect controlled variables (such as flow rate, rotational speed, weight, etc.) from the controlled object and send the detected signals back to the controller. The controller compares the feedback values with setpoints to calculate deviation errors, then generates corresponding control signals based on preset control algorithms. Upon receiving the control signals, actuators adjust control variables (such as valve opening, motor speed, vibration frequency, etc.) to affect the controlled object, dynamically driving the controlled variables toward their setpoints. This process achieves automatic system regulation and precise control (*Fowler et al., 2013)*.

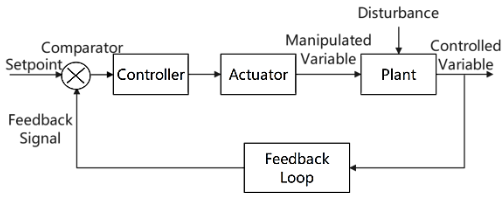

Fig. 10 – Block diagram of the closed-loop control system

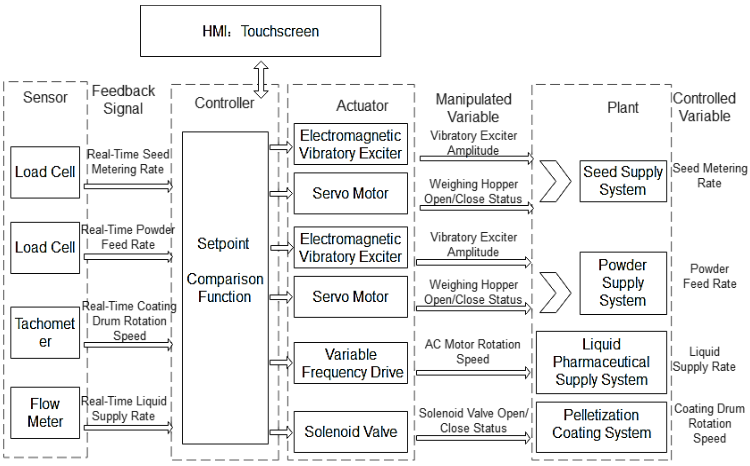

Fig. 11 – Schematic diagram of the control system

Based on the structural characteristics and operational workflow of the feeding device and pelleting-coating unit, the overall control system architecture was developed, as shown in Figure 11. This architecture includes a human-machine interface (touch screen), a controller (Microcontroller Unit), sensors (load cell, flow meter, speed sensor), actuators (electromagnetic vibrator, servo motor, solenoid valve, frequency converter), and controlled objects (seed feeding system, powder feeding system, liquid feeding system, and pelleting-coating system). The system achieves coordinated multi-subsystem control and integrated operation *(Du et al., 2025)*.

RESULTS AND DISCUSSION

Experimental Study on the Seed Supply Device

In this study, using Caragana seeds as test specimens, the focus was on analyzing the seeding speed and accuracy of the testing equipment. The experiment required the determination of two key parameters: resistance values corresponding to high/low seeding speeds and the optimal speed switching point (expressed as a percentage of the total seed quantity). The high-speed mode primarily enhances throughput, while the low-speed mode improves dosing accuracy. The speed switching point represents a critical control parameter for error reduction: excessively high values may cause airborne seeds to exceed the remaining quantity before switching, compromising accuracy; excessively low values prolong the process duration due to slower low-speed discharge of substantial residual seeds.

To analyze the seed feeding rate and error, the resistance (*RX*) in Figure 6 was adjusted from 0 to 1000 kΩ, with resistance values partitioned at 40 kΩ intervals. At each resistance setting, five replicate speed measurements were performed, and the mean value was calculated to generate the seed feeding rate variation curve corresponding to different resistance values, as illustrated in Figure 12.

As demonstrated by the test results in Figure 12, the seed feeding rate exhibited a downward trend with increasing resistance values. Within the resistance range of 0 to 440 kΩ, the feeding rate remained relatively stable above 50 g/s. Considering the maximum uniform coating capacity of the pelletization coating drum (200 g of seeds), the resistance value corresponding to the high-speed mode was selected as 480 kΩ, yielding a feeding rate of 42.61 g/s. This configuration balances rapid seed delivery and operational stability, effectively meeting the demands of high-throughput pelletization processes.

To mitigate seed feeding error by selecting resistance values in the low-speed mode, a focused investigation into error characteristics at high resistance values was conducted. A resistance range of 920 kΩ to 1000 kΩ (corresponding to seed feeding rates of 1.18 g/s to 4.33 g/s) was tested. The resistance values were partitioned at 10 kΩ intervals, with five replicate measurements performed at each interval. The mean value of these measurements was adopted as the error result for the respective resistance value. This methodology yielded the error variation curve corresponding to different resistance values, as shown in Figure.13.

As demonstrated by the experimental results in Figure 13, the error exhibited a decreasing trend with increasing resistance values. Combined with the seed feeding rate data from Figure 12, at a resistance value of 1000 kΩ, the corresponding seed feeding rate was 1.18 g/s with an error of 1.32 g. Both the feeding rate and error at this resistance value met the design requirements. Therefore, 1000 kΩ was selected as the optimal resistance value for the low-speed mode.

To investigate the influence of different seed feeding rate switching points on dosing accuracy, resistance values of 480 kΩ (high-speed mode) and 1000 kΩ (low-speed mode) were selected for a 200 g seed dosing error test. The switching points were set at 75%, 80%, 85%, 90%, and 95% of the target seed quantity. At each switching point, five replicate measurements were conducted. The mean error and standard deviation for each switching point were calculated, yielding the error variation curve corresponding to different switching points, as shown in Figure 14.

According to the experimental results shown in Figure 14, the seeding error reaches its minimum value with the smallest standard deviation when the seed feeding speed switching point is set at 90% of the total seed feeding amount, indicating optimal seeding stability under this condition. Therefore, 90% of the seed feeding amount is selected as the optimal switching point for seed feeding speed adjustment.

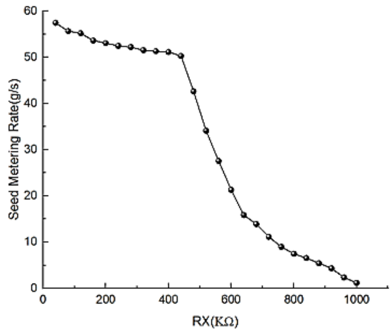

Fig. 12 – Variation curves of seed feeding speed under different resistance values

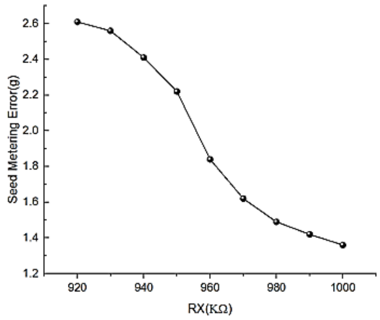

Fig. 13 – Variation curves of seed feeding error under different resistance values

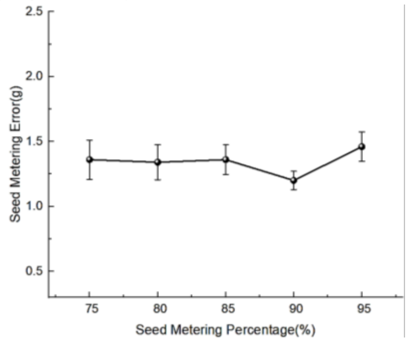

Fig. 14 – Variation curves of seed feeding error at different speed switching points

Experimental Study on the Powder Supply Device

Given the identical hardware design between the powder feeding device and the seed feeding device, the parameters requiring determination in the experiments are the same: the resistance value (*RX*) of the phase-shifting network and the powder feeding speed switching point (percentage of powder feed amount). To analyze the relationship between feeding speed and error, *RX* was set within the range of 260-680 kΩ, with resistance values partitioned at 20 kΩ intervals. For each resistance value, five speed measurements were conducted, and the average values were calculated to derive the powder feeding speed variation curve corresponding to different *RX* values, as shown in Figure 15.

As evidenced by the experimental results in Figure 15, the powder feeding speed exhibits a declining trend with increasing resistance values. When the resistance exceeds 520 kΩ, the rate of speed reduction accelerates markedly. Considering the total powder supply amount of 30 g in this study, the resistance value corresponding to the high-speed setting was selected as 260 kΩ, where the feeding speed reaches 2.41 g/s, thereby fulfilling the requirement for rapid powder delivery.

To reduce powder feeding errors by selecting resistance values under the low-speed setting, a focused investigation into error characteristics at high resistance values was conducted. Resistance values ranging from 920 kΩ to 1000 kΩ (corresponding to feeding speeds of 0.17 g/s to 0.46 g/s) were systematically tested. The resistance values were partitioned at 10 kΩ intervals, and five repeated measurements were conducted at each resistance value, with the average value adopted as the representative error result. This methodological framework yielded the powder feeding error variation curve corresponding to different resistance values, as illustrated in Figure 16.

As demonstrated by the experimental results in Figure 16, the powder feeding error exhibits a declining trend with increasing resistance values. Combined with the seed feeding speed data from Figure 15, at a resistance value of 600 kΩ, the corresponding powder feeding speed is 0.28 g/s, with a feeding error of 0.29 g. Both the feeding speed and error at this resistance value meet the design requirements. Therefore, 600 kΩ is selected as the optimal resistance value under the low-speed setting.

To investigate the influence of different powder feeding speed switching points on feeding accuracy, resistance values of 260 kΩ (high-speed setting) and 600 kΩ (low-speed setting) were selected for 30 g powder feeding accuracy tests. The switching points were set at 75%, 80%, 85%, 90%, and 95% of the total powder feeding amount. Five repeated measurements were conducted at each switching point. The average error values and standard deviations were calculated for each switching point, yielding the powder feeding error variation curve corresponding to different switching points, as shown in Figure 17.

As evidenced by the test results presented in Figure 17, the powder feeding error reaches its minimum value when the speed switching point is set at 85% of the total powder feeding amount. Notably, this configuration also yields the smallest standard deviation, demonstrating optimal feeding stability under these conditions. Based on these findings, 85% of the total powder feeding amount was determined to be the optimal speed switching point for the system.

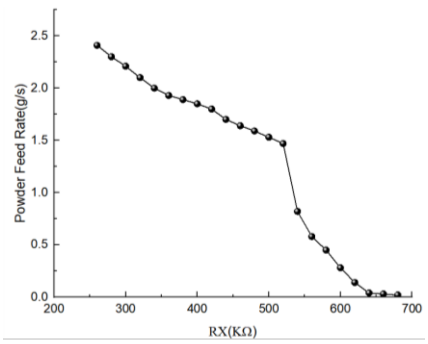

Fig. 15 – Variation curves of powder feeding speed under different resistance values

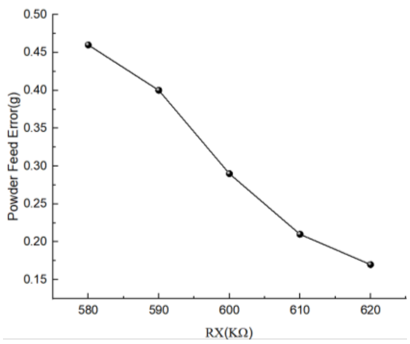

Fig. 16 – Variation curves of powder feeding error under different resistance values

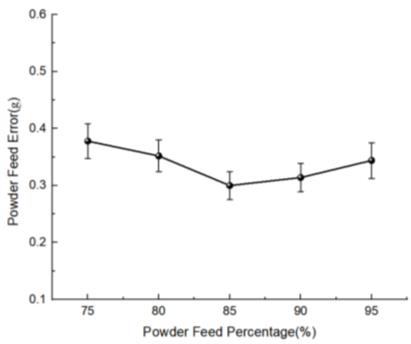

Fig. 17 – Variation curves of powder feeding error at different speed switching points

Error Test Testing

To verify whether the designs of the seed-feeding and powder-feeding devices meet the error requirements for coating operations, error analysis tests were conducted for both systems. The results of the seed-feeding error test are presented in Table 1, while the results of the powder-feeding error test are shown in Table 2.

Table 1

Seed Metering Error Test Value

SEED METERING QUANTITY [G]	NUMBER OF TRIALS	AVERAGE SEED DISPENSED [G]	ABSOLUTE ERROR [G]
100	5	101.2	1.2
150	5	151.16	1.16
200	5	201.16	1.16
250	5	251.1	1.1
300	5	301.18	1.18

Table 2

Powder Feeding Error Test Value

POWDER FEEDING QUANTITY [G]	NUMBER OF TRIALS	AVERAGE POWDER DISPENSED [G]	ABSOLUTE ERROR [G]
20	5	20.32	0.32
25	5	25.31	0.31
30	5	30.29	0.29
35	5	35.3	0.3
40	5	40.3	0.3

Based on the statistical calculations of the experimental data (n=5 trials), the systematic errors showed a gradual decrease with the increase of material quality. Specifically, the seed supply error gradually decreased from 1.2% to 0.39% (100-300 g interval), and the flour supply error decreased from 1.6% to 0.75% (20-40 g interval). Compared to the existing state-of-the-art systems, the maximum seed supply error in this study was reduced by 32% (from 1.8% to 1.2%) and the powder supply error was reduced by 53% (from 2.0% to 0.75%) compared to the benchmark study by *Zhang et al. (2022)*. The team reported seed supply/powder supply errors of 1.25-1.8% vs. 1.6-2.0%, respectively, under the same working conditions. The above performance improvement is due to the optimized layered switching control strategy, which effectively suppresses the inertial drop of the airborne residual material after the load cell triggers the closing of the drop plate.

CONCLUSIONS

This study developed a fully automated intelligent control system that integrates seed feeding, powder feeding, liquid supply, and coating functions to meet the specific process requirements of small grass seed pelleting and coating. The modular design of the system enables real-time monitoring and segmented adjustment of coating parameters through multi-sensor data fusion and hierarchical switching control, significantly enhancing the consistency of quality and the controllability of the pelleting and coating process for small seeds.

1) The study designed the seed-feeding and powder-feeding devices using a dual-mode control strategy, while employing a closed-loop control approach for the liquid-feeding device. The design was optimized to enhance the feeding accuracy of both the seed and powder delivery systems.

2) This study successfully integrated the control system with the pellet coating equipment and performed systematic performance validation tests. The experimental results show that the system achieves a seed feeding accuracy error of ≤1.2 g and a powder feeding accuracy error of ≤0.32 g, both of which meet the design specifications.

In order to further expand the application value of the system, the subsequent research can focus on the following directions:

1) optimization of multi-species adaptability: verify the system's adaptability to the coating of quinoa, sesame and other seeds with ultra-small particle sizes (Φ<1 mm), and develop parameter self-matching algorithms.

2) industrialization expansion research: design modular expansion interface, support multi-machine cooperative operation and flexible capacity configuration (50-500 kg/h), to adapt to the needs of large-scale production lines.

This technology can also be extended and applied in the field of precision powder engineering, such as pharmaceutical micro-pill coating, functional fertilizer preparation, etc., to provide technical support for the upgrading of agricultural intelligent manufacturing equipment.

ACKNOWLEDGEMENT

The authors were funded for this project by the Development and Research on Key Technologies and Equipment for Degraded Grassland Restoration Based on Coated Forage Seed Hydroseeding (No. 2023YFDZ0006) and the Science and Technology Research Project of Inner Mongolia Autonomous Region Higher Education Institutions (No.NJZZ23046).

REFERENCES

[1] Afzal, I., Javed, T., Amirkhani, M., & Taylor, A. G. (2020). Modern Seed Technology: Seed Coating Delivery Systems for Enhancing Seed and Crop Performance. *Agriculture*, Vol. 10(11), pp. 110526. https://doi.org/10.3390/agriculture10110526

[2] Campos, N., & Sanchez, A. (2012). Towards the Formal Implementation of Hierarchical Discrete-event Controllers in Automated Manufacturing Systems. *IFAC Proceedings Volumes*, Vol. 45, Issue 6, pp. 224-229. https://doi.org10.3182/20120523-3-RO-2023.00138

[3] Chandravanshi, M. L., & Mukhopadhyay, A. K. (2017). Dynamic analysis of vibratory feeder and their effect on feed particle speed on conveying surface. *Measurement*, Vol. 101, pp. 145-156. https://doi.org/10.1016/j.measurement.2017.01.031

[4] Despotović, Ž. V., Urukalo, D., Lečić, M. R., & Ćosić, A. (2017). Mathematical modeling of resonant linear vibratory conveyor with electromagnetic excitation: simulations and experimental results. *Applied Mathematical Modelling*, Vol. 41, pp. 1-24. https://doi.org/10.1016/j.apm.2016.09.010

[5] Du, Z., Yang, L., Zhang, D., Cui, T., He, X., Xie, C., Jiang, Y., Zhang, X., Mu, J., Wang, H., Xiao, T., & Li, H. (2025). Design and experiment of a soil organic matter sensor-based variable-rate seeding control system for maize. *Computers and Electronics in Agriculture*, Vol. 229, pp. 109752. https://doi.org/10.1016/j.compag.2024.10975.

[6] Fowler, A. G., Rakotondrabe, M., & Moheimani, S. O. R. (2013). Closed-Loop Control of a Novel 2-DOF MEMS Nanopositioner with Electrothermal Actuation. *IFAC Proceedings Volumes*, Vol. 46, Issue 5, pp. 391-398. https://doi.org/10.3182/20130410-3-CN-2034.00115

[7] Gai, W., & Wang, H. (2013). Closed-loop dynamic control allocation for aircraft with multiple actuators. *Chinese Journal of Aeronautics*, Vol. 26, Issue 3, pp. 676-686. https://doi.org/10.1016/j.cja.2013.04.031

[8] Jarrar, H., El-Keblawy, A., Ghenai, C., Abhilash, P. C., Bundela, A. K., Abideen, Z., & Sheteiwy, M. S. (2023). Seed enhancement technologies for sustainable dryland restoration: Coating and scarification. *Science of the Total Environment*, Vol. 904, pp. 166150. https://doi.org/10.1016/j.scitotenv.2023.166150

[9] Javed, T., Afzal, I., Shabbir, R., Ikram, K., Saqlain Zaheer, M., Faheem, M., Haider Ali, H., & Iqbal, J. (2022). Seed coating technology: An innovative and sustainable approach for improving seed quality and crop performance. *Journal of the Saudi Society of Agricultural Sciences*, Vol. 21, Issue 8, pp. 536-545. https://doi.org/10.1016/j.jssas.2022.03.003

[10] Ma, X., Liu, M., Hou, Z., Gao, X., Bai, Y., & Guo, M. (2023). Numerical simulation and experimental study on the pelletized coating of small grain forage seeds (小粒牧草种子丸粒化包衣数值模拟与试验). *Transactions of the Chinese Society of Agricultural Engineering*, Vol. 39, Issue 2, pp 43-52. DOI: 10.11975/j.issn.1002-6819.202211002

[11] Mucchi, E., Di Gregorio, R., & Dalpiaz, G. (2013). Elastodynamic analysis of vibratory bowl feeders: Modeling and experimental validation. *Mechanism and Machine Theory*, Vol. 60, pp. 60-72. https://doi.org/10.1016/j.mechmachtheory.2012.09.009

[12] Paravar, A., Piri, R., Balouchi, H., & Ma, Y. (2023). Microbial seed coating: An attractive tool for sustainable agriculture. *Biotechnology Reports*, Vol. 37, pp. e781. https://doi.org/10.1016/j.btre.2023.e00781

[13] Pasha, M., Hare, C., Ghadiri, M., Gunadi, A., & Piccione, P. M. (2017). Inter-particle coating variability in a rotary batch seed coater. *Chemical Engineering Research and Design*, Vol. 120, pp. 92-101. https://doi.org/10.1016/j.cherd.2017.01.033

[14] Pedrini, S., Webber, Z., D'Agui, H., Dixon, K., Just, M., Arya, T., & Turner, S. (2023). Customise the seeds, not the seeder: Pelleting of small-seeded species for ecological restoration. *Ecological Engineering*, Vol. 196, pp. 107105. https://doi.org/10.1016/j.ecoleng.2023.107105

[15] Sang, J., Zhao, C., & Zhu, C. (2015). Design of detection and control system for BY-150 seed coating machine (BY-150 型种子包衣机检测控制系统设计). *Transactions of the Chinese Society of Agricultural Machinery*, 37(3), 83-86. https://doi.org/10.13427/j.cnki.njyi.2015.03.020

[16] Upasan, A., & Kumsuwan, Y. (2013). Closed Loop Speed Control of Induction Generator with Scalar-control Inverters. *Energy Procedia*, Vol. 34, pp. 371-381. https://doi.org/10.1016/j.egypro.013.06.765

[17] Yang, W., Zhao, W., & Yang, M. (2014). Development of intelligent seed coating machine control system based on expert system (基于专家系统的智能化种子包衣机控制系统研制). *Journal of Chinese Agricultural Mechanization*, Vol. 35, Issue 1, pp. 216-219+248

[18] Yi, L. (2020). Problems and countermeasures of grass seed coating technology (草种子包衣技术存在问题及对策). *Chinese Journal of Animal Husbandry and Veterinary*, vol. 12, pp. 193-194

[19] Zhang, X., Huang, Y., Wang, S., Jiang, L., Li, G., & Xie, Y. (2021). Hierarchical autonomous switching control of a multi-modes omnidirectional mobile robot. *Mechatronics*, Vol. 80, pp. 102692. https://doi.org/10.1016/j.mechatronics.2021.102692

[20] Zheng, X., Huang, J., Li, Y., Wan, L., Ma, X., Song, J., & Liu, Z. (2024). Numerical simulation method of seed pelletizing: Increasing seed size by powder adhesion. *Powder Technology*, Vol. 444, pp. 119991. https://doi.org/10.1016/j.powtec.2024.119991

[21] Zhang, X., Hou, Z., & Dai, N. (2022). Design of an Electric Control System for Seed Coating Based on LabVIEW (基于 LabVIEW 的种子包衣电控系统的设计). Journal of Chinese Agricultural Mechanization, Vol. 44, Issue 7, pp. 112-117. DOI:10.13427/j.cnki.njyi.2022.07.019.